

PPPL Calculation Form - No: NSTXU-CALC-133-23 #

Calculation # NSTXU-CALC-133-23 Revision # 0 WP #, if any 2254
(ENG-032)

Purpose of Calculation: (Define why the calculation is being performed.)

The purpose of this calculation is to obtain the maximum poloidal magnetic fields from an axis-symmetric global electromagnetic (EM) model with winding pack details for six inner PFs but smeared properties used for all other PF and OH coils in the global EM model setup. The global EM analysis includes magnetostatic simulations under normal operations for various load cases such as with and without (shaped or circular) plasmas, post disruptions, scanned through the 96 equilibrium scenarios defined in the GRD, plasma VDEs as well as the suppress and bypass case where overcurrent on coils is induced on the inner PFs during shutdown transients.

Codes and versions: (List all codes, if any, used)

ANSYS 18.2

References (List any source of design information including computer program titles and revision levels.)

- [1] NSTX-U-RQMT-GRD-001-00 General Requirements Document, S. Gerhardt, December, 2017
- [2] NSTX-U-RQMT-SRD-002-00 System Requirements Document Magnet Systems, S. Gerhardt, December, 2017.
- [3] Inner PF coil design parameters, M. Kalish, February, 2018.
- [4] NSTX-CRIT-0001-02 Structural Design Criteria, I. Zatz, January, 2016.
- [5] Design Point Spreadsheet NSTX_CS_Upgrade_120409, C. Neumeyer, April, 2012.
- [6] NSTX-U-SPEC-MAG-001-2 Specification for Inner PF coil conductor, M. Kalish, November, 2017
- [7] Stress Analysis of Inner PF Coils (1a, 1b & 1c), Center Stack Upgrade, L. Myatt, April, 2012.
- [8] Inner-PF Coil Interfaces to Supports Designs and Cooling Systems, NSTX-U_RQMT-RD-012-00, S. Gerhardt, March, 2018.
- [9] Material Properties for Inner PF Coil FDR, MAG-180306-YZ-01, Y. Zhai, March, 2018.
- [10] Calculation of Suppress/Bypass Shutdown Currents for Inner PF Coils, C. Neumeyer, NSTX-U-CALC-52-01-00, March 6, 2018.
- [11] Calculation of Inner PF Coil Leads and Bus Bars, Y. Zhai, T. Willard, W. Wang and A. Khodak, NSTX-U-CALC-133-24-00, March 18, 2018.
- [12] Inner PF Coil Thermal Analysis, Y. Zhai, NSTX-U-CALC-133-27-00, March 14, 2018.
- [13] Calculation of Suppress and Bypass Currents and Coil Response, C. Neumeyer, NSTX-U-CALC-CC-52-00, March, 2018.
- [14] Calculation of Suppress and Bypass Coil and Bus Dynamic Structural Response, P. Titus, NSTX-U-CALC-55-11, March 14, 2018.

Assumptions (Identify all assumptions made as part of this calculation.)

The global electromagnetic (EM) and inner PF winding pack structural analysis is performed with 2D axis-symmetric models established previously but using the latest inner PF coil design parameters to model the winding pack details of inner PFs. Current inputs for the EM analysis are the 96 EQ scenarios given in the Design Point Spread Sheet. A 2D global EM model with all PF and OH coils is used for a magneto-static analysis, followed by a static structural analysis for the inner PFs using the same axis-symmetric model with winding pack details for the PF-1a, PF-1b and PF-1c coils. This report is to summarize the results from the 2D EM and structural calculation of coil winding packs for validating the new design of the inner PF coils.

Calculation (Calculation is either documented here or attached)

Please see attached main body of this document.

Conclusion (Specify whether or not the purpose of the calculation was accomplished.)

The main conclusions include

1. *The conductor static and fatigue stresses meet the NSTX-U structural design limits. The insulation shear and compressive stresses meet the design allowable for all 96 EQ scenarios with additional 10% headroom on the PF coil currents.*
2. *The worst case EQ scenarios in terms of maximum local magnetic fields and stresses in coil winding packs for PF-1a, PF-1b and PF-1c coils are EQ#1 & 51, EQ #33 and EQ #18 respectively.*
3. *Plasma disruptions and post-disruption events, as well as Vertical Displacement Events (VDEs), shall be considered as normal events, only PF-1c coils have 5% overall currents during post-disruptions from the 96 EQ scenarios, which is much lower than the stress margins for the PF-1c coils. The field and stress change due to worst case VDEs will not be an issue for the inner PFs.*

Although the new design with a spiral winding of inner PF solenoids is much better in terms of field symmetry than the previous design with joggles in the winding, the 3D impact of coil spiral winding to net Lorentz forces, error fields, and the magnetic centers is not included in the 2D calculation. A complete 3D analysis using ANSYS MAXWELL has been performed for each of the inner PFs with spiral winding of coils, lead flags and bus bars. The results are reported in the leads and bus bar analysis.

Cognizant Individual (or designee) printed name, signature, and date

Steve Raftopoulos

Digitally signed by Steve Raftopoulos
Date: 2018.09.11 15:45:56 -04'00'

Preparer's printed name, signature and date

Yuhu Zhai

Digitally signed by Yuhu Zhai
Date: 2018.09.11 15:24:07 -04'00'

I have reviewed this calculation and, to my professional satisfaction, it is properly performed and correct.

Checker's printed name, signature, and date

Art Brooks

Digitally signed by Art Brooks
Date: 2018.09.11 15:28:57 -04'00'



National Spherical Torus eXperiment - Upgrade

NSTX-U

Inner PF Coil Electromagnetic Analysis

NSTXU-CALC-133-23 - Rev 0

March 30, 2018

Yuhu Zhai Digitally signed by Yuhu Zhai
Date: 2018.05.15 08:38:41
-04'00'

Yuhu Zhai

Prepared By

Your name here

Art Brooks Digitally signed by Art Brooks
Date: 2018.05.15 09:06:56
-04'00'

Art Brooks

Reviewed By

Reviewers name here

Michael Kalish Digitally signed by Michael Kalish
DN: cn=Michael Kalish, o=PPPL,
ou=Engineering, email=mkalish@pppl.gov,
c=US
Date: 2018.05.15 09:01:43 -04'00'

Mike Kalish

Approved By – Responsible Engineer

Responsible Engineer's name here

NSTX-U Calculation Form

Purpose of Calculation: The NSTX-U inner PF coils are water-cooled copper solenoids fabricated from rectangular or square shaped conductors with embedded central cooling channels. The inner PFs, consist of three upper and lower coil pairs, denoted PF-1a, PF-1b and PF-1c, are energized up to 20 kA for about 1-2 seconds during plasma operations and then cooled down with 12 °C cold water once every 1200 seconds. The inner PFs are designed to have 20,000 pulse cycles in which conductors for all six coils will experience the primary stress under Lorentz forces during machine operations. This calculation is to obtain the maximum poloidal magnetic fields from an axis-symmetric global electromagnetic model with winding pack details for six inner PFs but smeared properties for all other PF and OH coils. The global electromagnetic analysis is followed by a 2D static structural analysis so to extract primary stresses in the conductor and turn insulation when coils are pulsed. The global EM analysis includes magnetostatics simulations under normal operations for various load cases, such as with and without (shaped or circular) plasmas, post disruptions, scanned through the 96 equilibrium scenarios defined in the GRD, Plasma Vertical Displacement Events (VDEs), as well as the suppress and bypass case where overcurrent on coils is induced on the inner PFs during shutdown transients. The results are evaluated for the inner PFs with winding pack details to ensure that conductor and insulation stress and strain is under the design limits per NSTX-U Structural Design Criteria. All 96 equilibrium scenarios from the DPSS are scanned in the process, and results are analyzed to extract the maximum magnetic fields and then peak stresses in the coil winding packs. The global EM model is also used for extracting the maximum local radial magnetic fields for the 3D structural analysis of coil lead sections and bus bars for the inner PFs. We conclude based on the result that conductor and insulation stress / strain meets the static and fatigue requirements for the inner PF design per NSTX-U General Requirements Document [1] and the System Requirements Document for Magnet Systems [2].

References:

[1] NSTX-U-RQMT-GRD-001-00 General Requirements Document, S. Gerhardt, December, 2017

[2] NSTX-U-RQMT-SRD-002-00 System Requirements Document Magnet Systems, S. Gerhardt, December, 2017.

[3] Inner PF coil design parameters, M. Kalish, February, 2018.

[4] NSTX-CRIT-0001-02 Structural Design Criteria, I. Zatz, January, 2016.

[5] Design Point Spreadsheet NSTX_CS_Upgrade_120409, C. Neumeyer, April, 2012.

- [6] NSTX-U-SPEC-MAG-001-2 Specification for Inner PF coil conductor, M. Kalish, November, 2017
- [7] Stress Analysis of Inner PF Coils (1a, 1b & 1c), Center Stack Upgrade, L. Myatt, April, 2012.
- [8] Inner-PF Coil Interfaces to Supports Designs and Cooling Systems, NSTX-U_RQMT-RD-012-00, S. Gerhardt, March, 2018.
- [9] Material Properties for Inner PF Coil FDR, MAG-180306-YZ-01, Y. Zhai, March, 2018.
- [10] Calculation of Suppress/Bypass Shutdown Currents for Inner PF Coils, C. Neumeyer, NSTX-U-CALC-52-01-00, March 6, 2018.
- [11] Calculation of Inner PF Coil Leads and Bus Bars, Y. Zhai, T. Willard, W. Wang and A. Khodak, NSTX-U-CALC-133-24-00, March 18, 2018.
- [12] Inner PF Coil Thermal Analysis, Y. Zhai, NSTX-U-CALC-133-27-00, March 14, 2018.
- [13] Calculation of Suppress and Bypass Currents and Coil Response, C. Neumeyer, NSTX-U-CALC-CC-52-00, March, 2018.
- [14] Calculation of Suppress and Bypass Coil and Bus Dynamic Structural Response, P. Titus, NSTX-U-CALC-55-11, March 14, 2018.

Assumptions: *(Identify all assumptions made as part of this calculation.)*

The global electromagnetic (EM) and inner PF winding pack structural analysis is performed with 2D axis-symmetric models established previously but using the latest inner PF coil design parameters to model the winding pack details of inner PFs. Current inputs for the EM analysis are the 96 EQ scenarios given in the Design Point Spread Sheet. A 2D global EM model with all PF and OH coils is used for a magneto-static analysis, followed by a static structural analysis for the inner PFs using the same axis-symmetric model with winding pack details for the PF-1a, PF-1b and PF-1c coils. This report is to summarize the results from the 2D EM and structural calculation of coil winding packs for validating the new design of the inner PF coils.

Calculation: *(Calculation is either documented here or attached)*

Contents

1. Executive Summary	5
2. Inner PF Coil Design	5
3. Structural Design Limits.....	7
4. Global EM Analysis.....	9
5. EM Results.....	11

1. Executive Summary

The inner PF coils for the NSTX-U are installed to provide the poloidal field shaping and better controlling of plasma in the diverter region during machine operations. The inner PFs, fabricated from rectangular or square-shape copper conductors with embedded central cooling channels, are designed to have 20,000 pulse cycles over the lifetime of machine operation as defined in the latest General Requirement Document [4]. The key design requirements for magnet operations include 1) all PF coils shall be capable of supplying 100% of their rated ampere-turns, including 10% engineering headroom, 2) all aspects of the PF coils design shall be compatible with NSTX-U operation with plasma current and toroidal field in either toroidal direction. To this end, 2D electromagnetic and structural coupled analyses were performed based on an axis-symmetric model of all PF and OH coils as well as shaped or circular plasma where detailed winding packs are included for the inner PF-1a, PF-1b and PF-1c coils to validate the coil design. The EM results from magnetostatics analysis show that the worst EQ scenarios are #1, 51, #33 and #18 for the PF-1a, -1b and -1c coils respectively. The maximum vertical fields on the conductors, when pulsed, are 2.5, 2.2 and 1.1 T for PF-1a, -1b and -1c coils respectively. The maximum radial fields are 2, 2.1 and 1.7 T for PF-1a, -1b and -1c respectively. Independent from the poloidal magnetic fields, which induce hoop stress and vertical forces in coil winding packs, toroidal fields are not included in the 2D EM analysis as they have little stress effect on the inner PF winding packs. The maximum toroidal fields are 2.9, 2.4 and 1.7 for PF-1a, -1b and -1c respectively. The coil primary stresses under the worst case Lorentz loads meet the conductor stress design requirement [4, 6]. A fatigue strength evaluation is required for structural components including conductors and insulations, with undetectable flaws that are either cycled over 10,000 times during their operational lives or are exposed to cyclic peak stresses exceeding its yield stress. A fatigue strength evaluation is performed for the 2D coil winding pack. As an important part of the coil design validation process, the fatigue strength evaluation includes meeting requirements of either the design Stress-N (S-N) fatigue curve derived from material test data, or the crack growth limitation for the 20,000 cycles.

2. Inner PF Coil Design

The coil geometry and conductor dimension of the global EM analysis models are taken from the latest Kalish Coil Design Parameter data sheet [3]. To ensure a self-consistent coil alignment with consideration of assembly and positional tolerances of components, the PF-1a conductor width was reduced by 1 mm since inner PF PDR so to increase the inner bore size by 8 mm (4 mm on each side), and cooling hole size is reduced from

0.225" to 0.185" accordingly so to maintain the same width from the hole edge to the conductor outer side edge for fatigue crack propagation of 1mm minimum detectable flaws. In Table 1, the Equivalent Square Wave (ESW) for PF-1a is reduced accordingly from 2.1s to 1.9s so to maintain the same maximum temperature with the conductor modification [2].

Table 1 – Inner PF Physics Requirements [2]

	PF-1a	PF-1b	PF-1c
No. of turns	61	20	16
Max current (kA)	19.67	20	20.25
ESW time (s)	1.9	1.0	1.4

Tables 2-3 listed the coil design parameters and the inner PF conductor dimensions [3], used as the input to establish the 2D axis-symmetric thermal analysis models. Figure 1 presents the inner PF coils in the polar region of NSTX-U, and the 2D cross section of the PF-1b used in the electromagnetic analysis model.

Table 2 – Inner PF Coil Design Parameters

		MK PF Coil Sizing 02-01-18					
		PF1A (")	PF1B (")	PF1C (")	PF1A (mm)	PF1B (mm)	PF1C
R center	$r_0=$	12.81	15.44	21.85	325.374	392.176	554.99
Z center	$z_0=$	62.62	71.03	71.4	1590.548	1804.16	1813.56
Coil ID	ID=	23.03	29.32	41.66	585	745	1058
Coil OD	OD=	28.21	32.44	45.74	717	824	1162
Width	w=	2.59	1.56	2.04	58.1152	31.9532	44.1452
Height	h=	18.44	7.17	6.94	468.376	174.447	168.605

Table 3 – Inner PF Conductor Dimension

Conductor	PF1A (")	PF1B	PF1C	PF1A (mm)	PF1B	PF1C
Width	0.481	0.54	0.78	12.2174	13.716	19.812
Height	0.98	0.5	0.61	24.892	12.7	15.494
hole	0.185	0.146	0.146	4.699	3.7084	3.7084

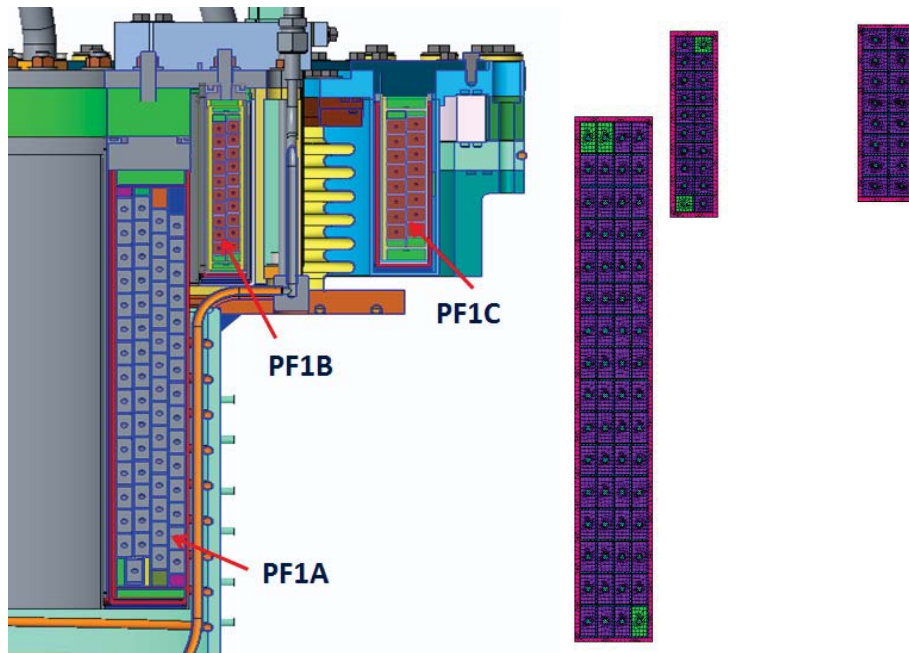


Figure 1 Inner PFs in Polar Region (left) and 2D Analysis Model of PF-1 (right)

3. Structural Design Limits

According to [4], fatigue S-N fatigue curves shall be obtained based on the uniaxial strain cycling tests at service temperatures and at various R ratios. S-N fatigue curves shall be developed for both the base metal and for braze joints in the coil lead region.

- a. The conductor static stress design limit is derived from the minimum yield strength given in the specifications for the inner PF conductors
- b. The fatigue limit for copper is derived from the copper fatigue S-N curve

Figure 2 presents the stress categorization from the structural design criteria, and the static and fatigue S-N curve from copper test data available from a number of references. For S-N fatigue evaluation, the more strict criteria of 2 on stress and 20 on life must be met. For the fracture mechanics evaluation, a factor of 2 on minimum detectable flaw size, 1.5 on fracture toughness, and 2 on life must be met. The measured NSTX OH conductor braze joint fatigue life is also included in the evaluation, along with the published S-N data for comparison.

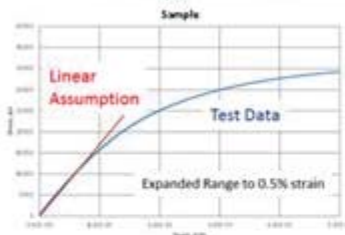
- *NSTX-U Structural Design Criteria*
 - Coils are evaluated by comparing Tresca stress to design limits
 - Main loads include EM (96 EQ) and Thermal during cool down

Stress Category	Parameters	Stress Intensity Limits
General primary membrane	P_m	$k S_m$
Local primary membrane	P_L	$1.5 k S_m$
Primary membrane plus bending	$(P_m + P_b)$ or $(P_L + P_b)$:	$1.5 k S_m$
Primary plus secondary	$(P_m + P_b + Q)$ or $(P_L + P_b + Q)$	$3 S_m$

- S_m - design stress limit, based on load cases
 - k -factor – Normal operation $k = 1.0$
 - Anticipated events $k = 1.1$
 - Unlikely events: $k = 1.2$

- *Static*

- S_m is the smaller of $2/3 \sigma_y$ or $1/2 \sigma_u$ at the service temperature



σ_y (MPa)	σ_u	S_m	$1.5*S_m$	$3*S_m$	Temperature
103	221	69	103	207	20 C
93	198	62	93	186	100 C

- *Fatigue* - Total cycles of 20,000 – *NSTX CSU Pulse Spectrum*

Criteria	Stress Level and Type	Actual
SN 2 on stress	112 MPa (Tresca)	142
SN 20 on life	180 (Tresca)	142
Fracture Mechanics with a flaw size less than .7mm 1.5 on K _{Ic} and 2 on Cycles	140 MPa (Max Principal or Hoop)	101
4 on cycles	125 MPa (Max Principal or Hoop)	101

[Conductor Fatigue and Fracture Mechanics Analyses](#)

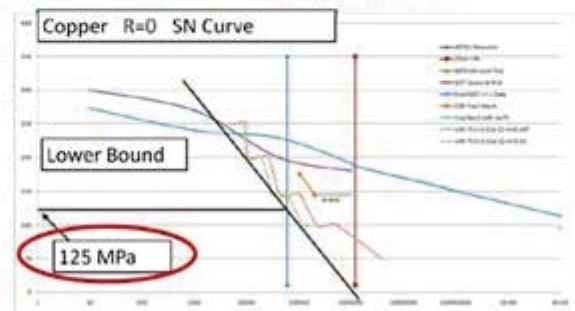


Figure 2 SN and Fracture Mechanics Fatigue Life

Figure 2 Structural Design Criteria and Conductor Static and Fatigue Limits

4. Global EM Analysis

Two-dimensional axis-symmetric ANSYS EM analysis model was developed including all the PF and OH coils where winding pack details for the PF1-a, PF1-b and PF1-c are included but smeared properties for all other PF and OH coils are used [7]. The 2D EM analysis models include the conductors, turn-to-turn and layer insulations, as well as the ground wrap insulations. Figure 3 presents the global EM model where both shaped or circular plasmas with detailed inner PFs and smeared OH and PF2-5 coils, as well as the infinite element domain used for the global magnetostatics analysis. Independent from the poloidal magnetic field systems, toroidal fields generated from the TF coils are not included in 2D analysis since they have little stress effect on the inner PF winding packs. Impact of the toroidal fields to the coil leads and bus bars, on the other hand, are addressed in the full 3D MAXWELL models and the results will be reported in a separate calculation [11].

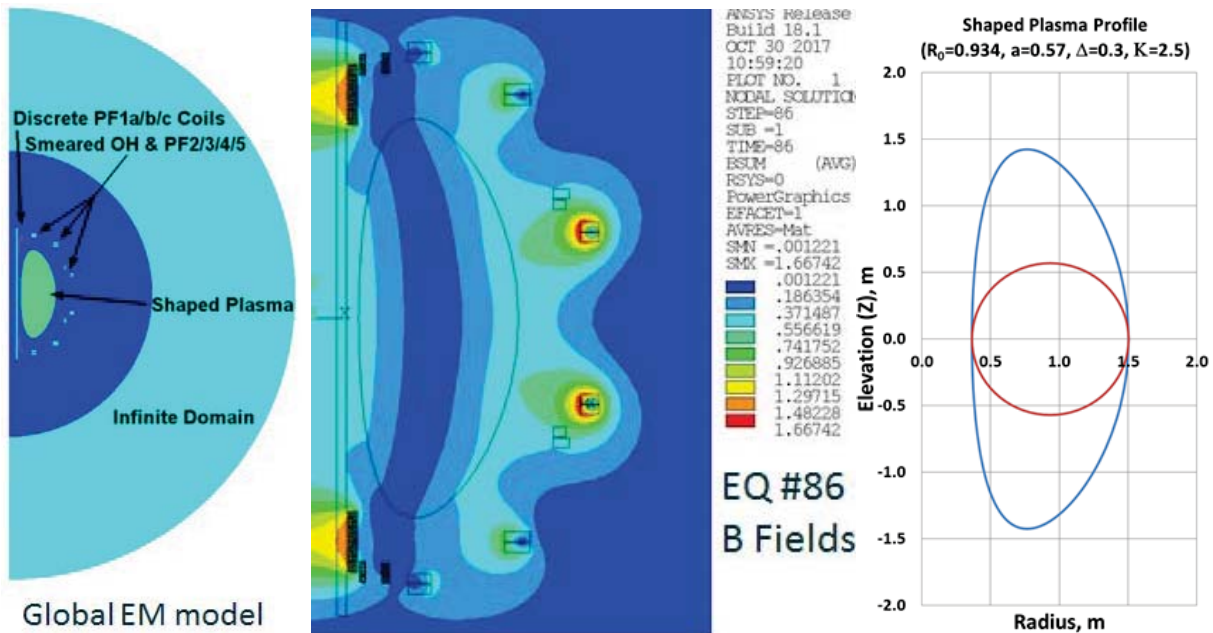


Figure 3 Global EM Analysis Model for Inner PFs, Magnetostatics

Table 4 – Plasma conditions for Inner PFs

	PF-1a	PF-1b	PF-1c
No plasma	#1, #52	#33, #34	#84
2 MA circular plasma	#51, 54	#18, 33	#18
2 MA shaped plasma			
Max centering force (klb)	89	49	33
Max launching force (klb)	52	79	45

Current requirements for the inner PFs are initially specified in the NSTX-U Design Point Spreadsheet (DPSS) based on the peak amp-turns from the 96 design-basis plasma equilibria [5]. The new inner PF design is intended to preserve the same flux generated to meet physics requirements on the flux swing. Although there are little changes in the total Ampere-turns, currents in the inner PFs from the new coil design are quite different as the result of changing number of turns. Table 5 represents a comparison of the new design vs the previous design described in the DPSS [5]. A current scaling factor is used on the coil EM analysis so to extract the maximum fields and stresses within the inner PF coil winding packs.

Table 5 – Design Change from DPSS and Current Scaling for Inner PFs

	NSTX-U			NSTX-U Recovery			NI scale factor	I scaling factor
	I (kA)	turns	I-t (kA)	I (kA)	turns	I-t (kA)		
1A	19	64	1216	19.6722	61	1200	1.013	1.035
1B	13	32	416	20	20	400	1.040	1.538
1C	16	20	320	20.25	16	324	0.988	1.266

Figures 4-5 present the coil currents for the upper and lower inner PFs [5]. The currents for the PF-1b and PF-1c are symmetric for the upper and lower coils, currents on the PF-1a coils, on the other hand, are un-symmetric for the upper and the lower coils (single null requirements). Higher currents are defined for the upper PF-1a for the EQ scenarios 34-62 as shown in the current plots below as the result of the single null divertor configuration.

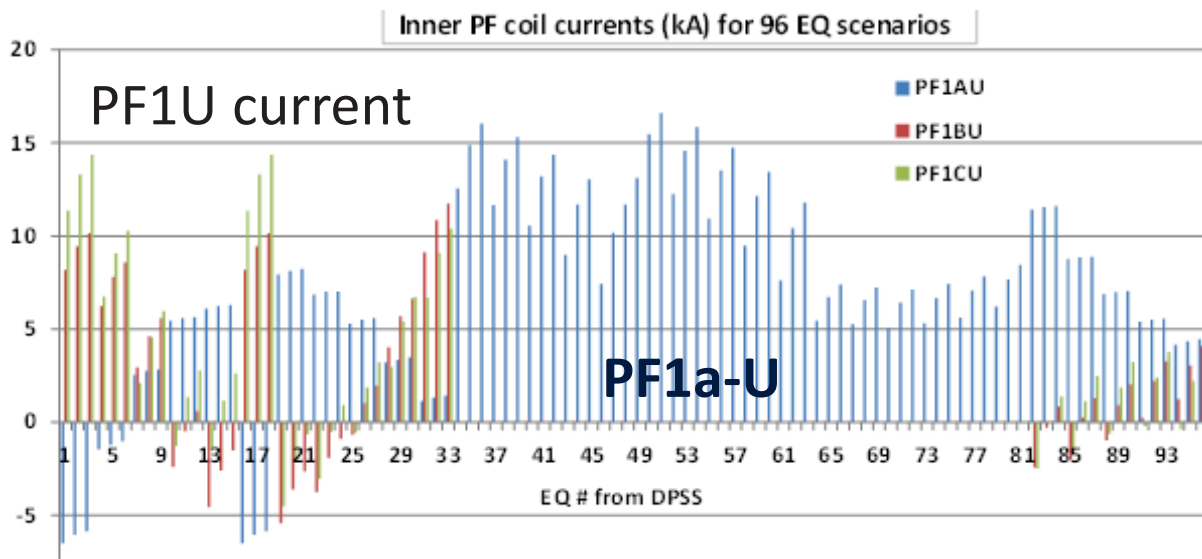


Figure 4 Inner PF Currents (upper) for the 96 Scenarios per DPSS

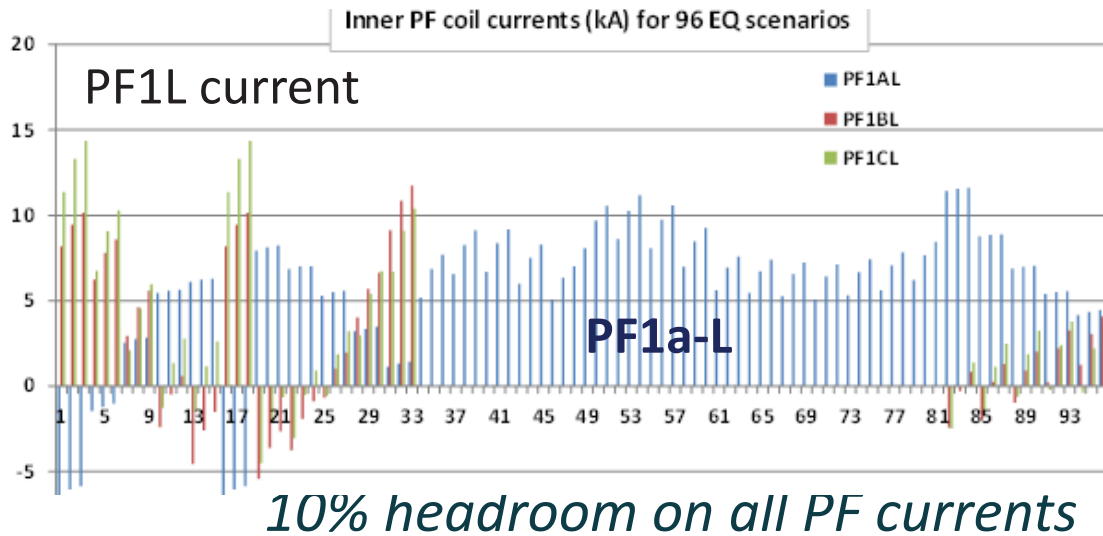


Figure 5 Inner PF Coil Currents (lower) for the 96 Scenarios per DPSS

5. EM Results

When the inner PFs are energized, the conductor will be pulsed up to ~20 kA for about 1-2 seconds. The conductor and insulation will experience primary fatigue stress and strain under the worst EM loads, but EM stress during operation dominates the fatigue evaluation for the conductor within the coil winding pack, and EM stress due to Lorentz loads (with toroidal fields) dominates the fatigue evaluation for coil leads. During normal operation, the equivalent square wave (ESW) time of PF-1a, -1b and -1c coils is 1.9, 1.0 and 1.4 seconds respectively.

Maximum Magnetic Fields and Coil Forces

The typical global magnetic fields in the PF winding packs are shown in Figures 6-8. The worst EQ scenarios for each inner PFs in terms of the maximum field on the coils are selected and resultant stresses or net forces out of all 96 EQ scenarios on inner PF coils are comparable with the DPSS. Figure 9 presents the poloidal field distributions on the inner PF coils during the worst case scenarios (10% headroom applied on all PF coil currents). Figures 10-11 present the maximum forces (vertical forces and radial forces) on the inner PFs. The worst net forces for 10 out of the all 96 EQ # were selected during Inner PF PDR are comparable with that from the Design Point Spread sheet (DPSS).

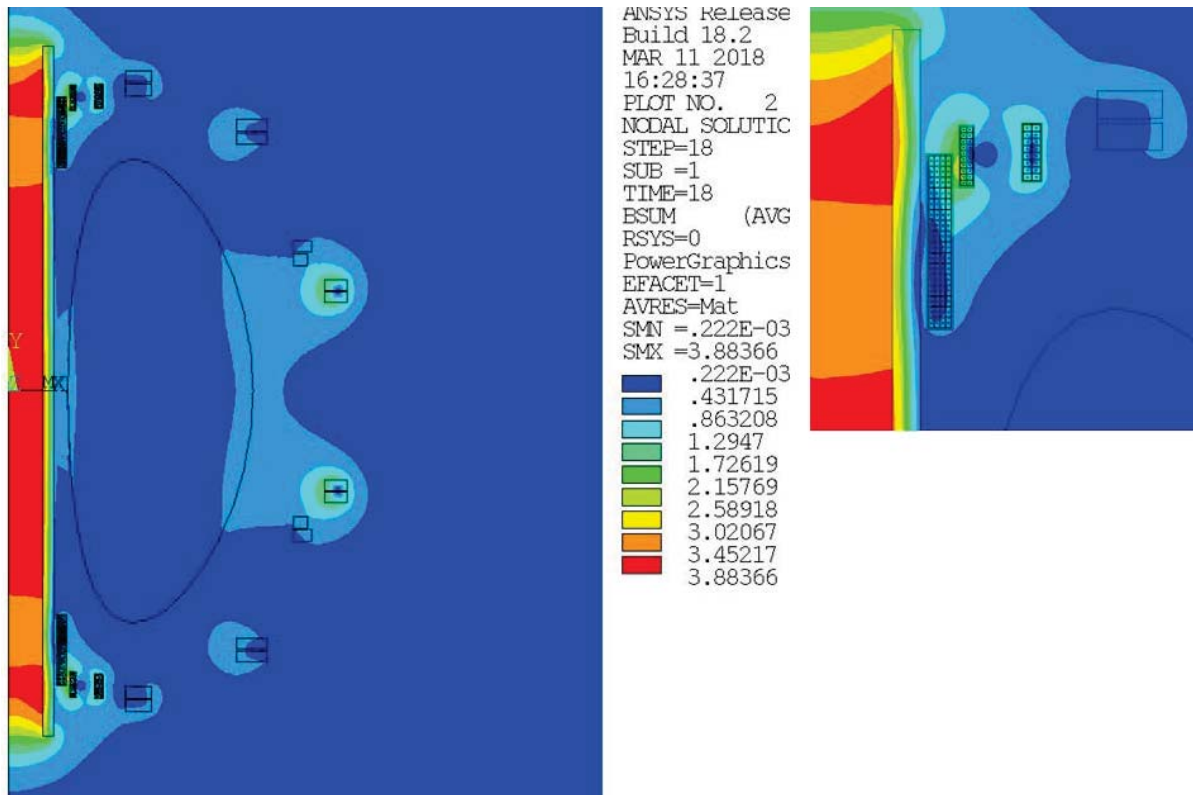


Figure 6 Global Poloidal Fields for Inner PFs, Magnetostatics EQ#18

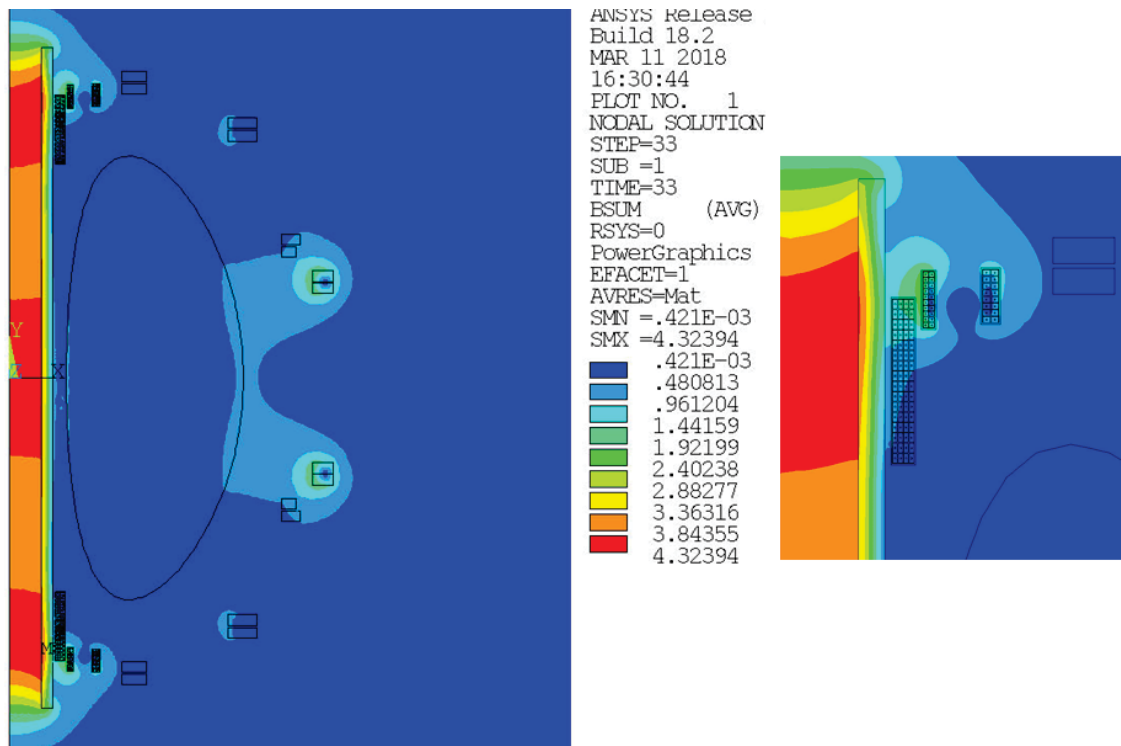


Figure 7 Global Poloidal Fields for Inner PFs, Magnetostatics EQ#33

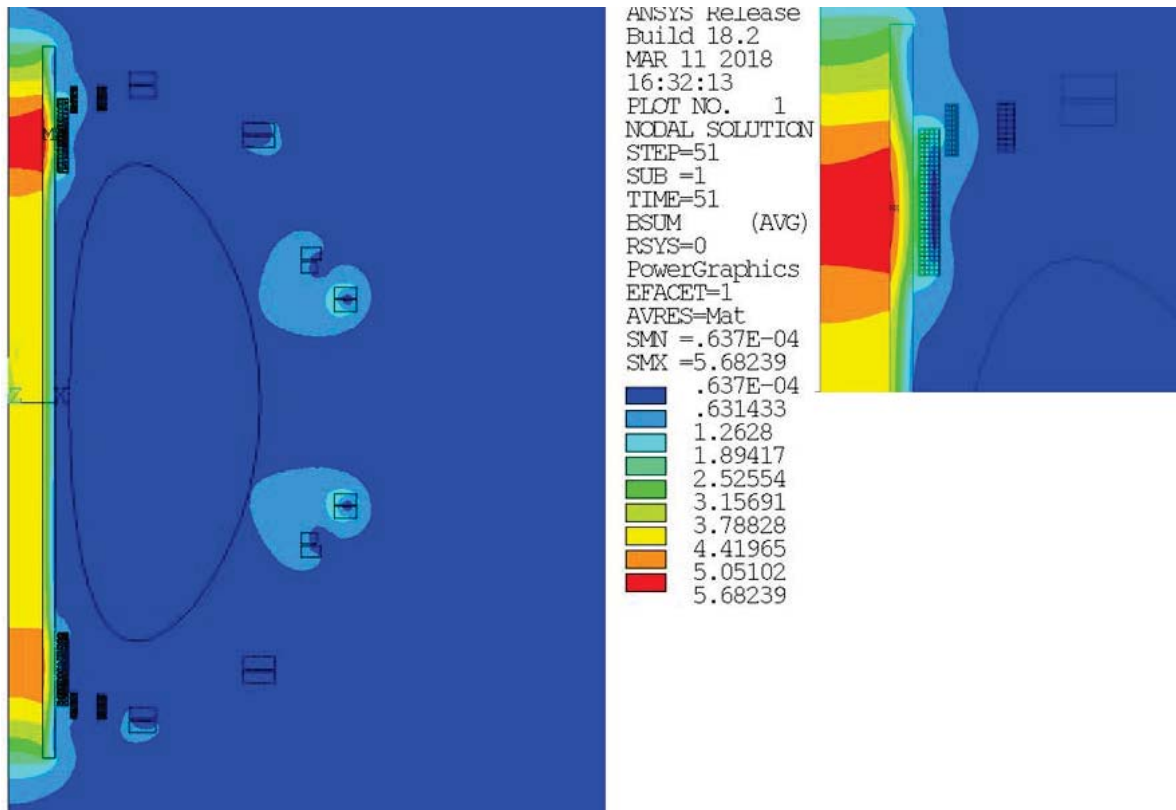


Figure 8 Global Poloidal Fields for Inner PFs, Magnetostatics EQ#51

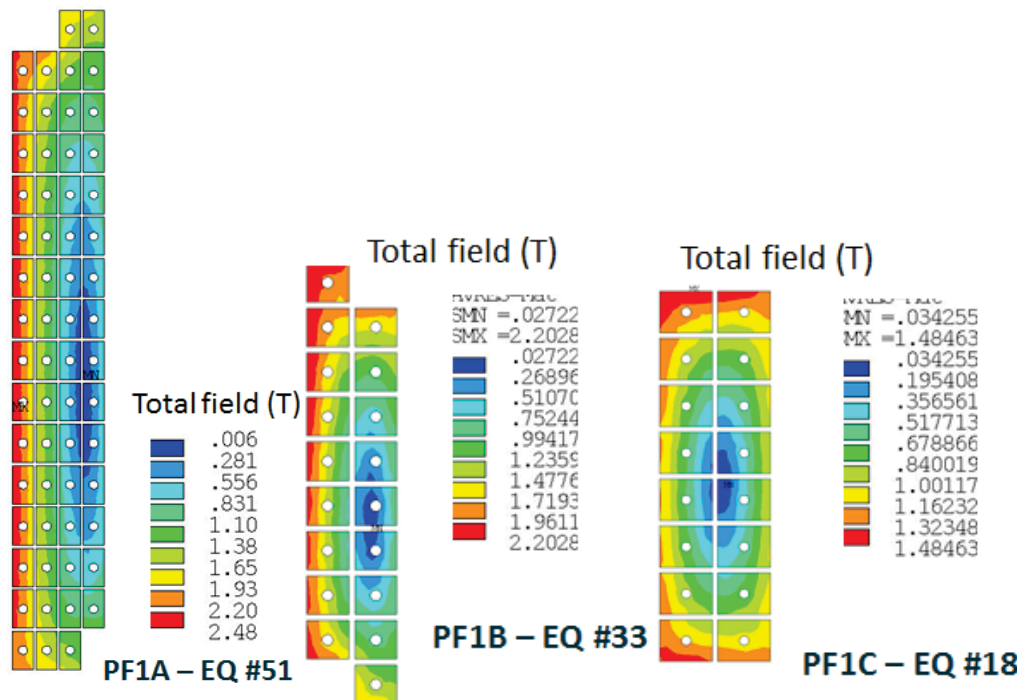


Figure 9 Poloidal Fields on the inner PFs for the worst EQ scenarios (10% head room applied on all PF coil currents)

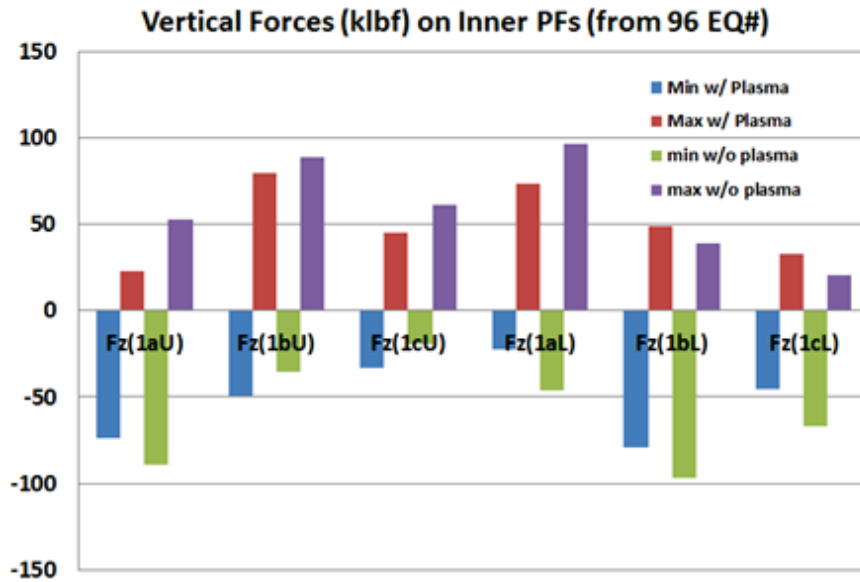


Figure 10 Maximum vertical forces on inner PF coils (out of all 96 scenarios).

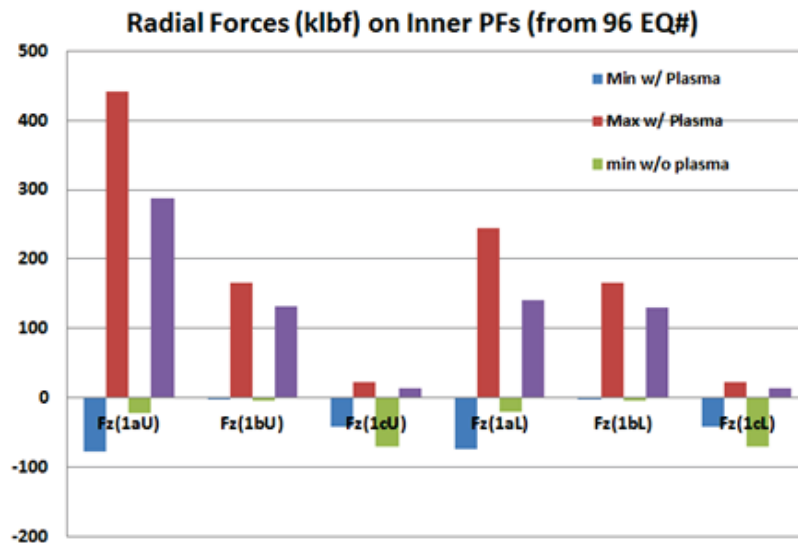


Figure 11 Maximum radial forces on inner PF coils (out of all 96 scenarios).

The typical radial and vertical forces on the upper and lower inner PFs are presented in Figure 12 and Figure 13 respectively. The conductor is hot at the end of the pulse as shown in the 2D thermal analysis [12]. Table 5 listed the maximum fields on the inner PFs under various worst load cases out of the 96 EQ scenarios. The toroidal fields are estimated based on the axial current filament in the center.

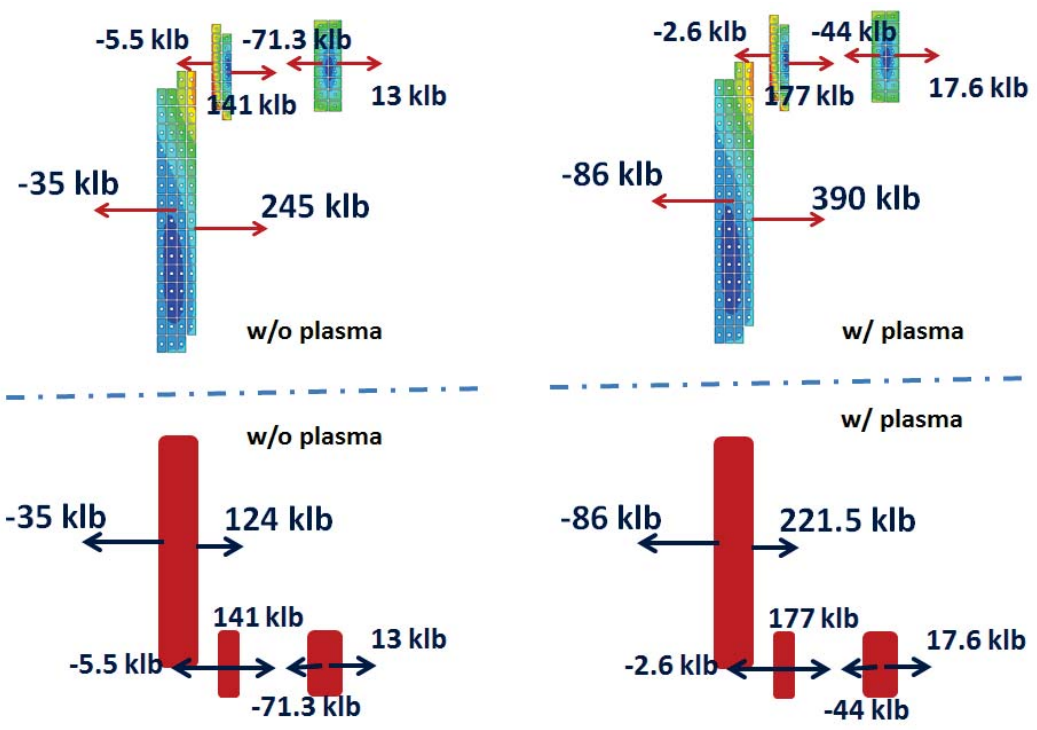


Figure 12 Typical radial forces on the upper and lower inner PFs.

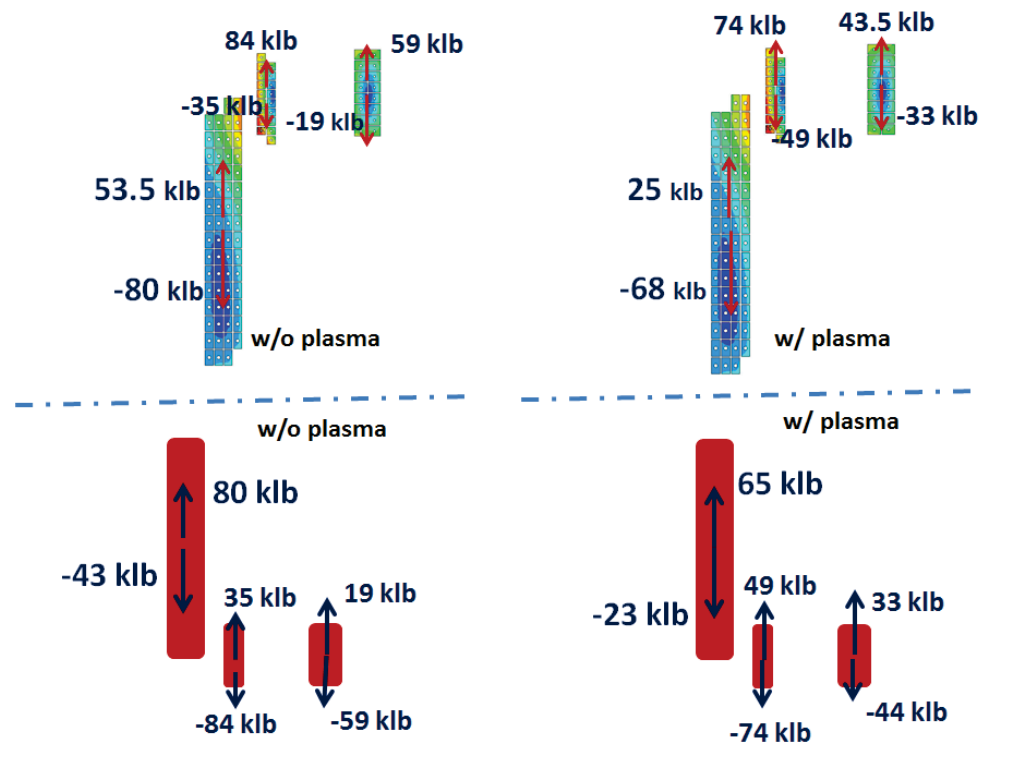


Figure 13 Typical vertical forces on the upper and lower inner PFs.

Table 6 – Maximum Fields on Inner PFs

	PF-1a	PF-1b	PF-1c
Worst EQ #	51	18, 33	18
Radial B_r (T)	2	2.1	1.7
Vertical B_z (T)	2.5	2.2	1.1
Toroidal B_t (T)	2.9	2.4	1.7

Full 3D EM analysis for each of the worst EQ scenarios has also been performed for the coil terminal and bus bar analysis [11]. Figure 14 shows the total field plot from EQ #51 and the field on the upper PF-1a coil spiral winding with bus bars from the 3D results.

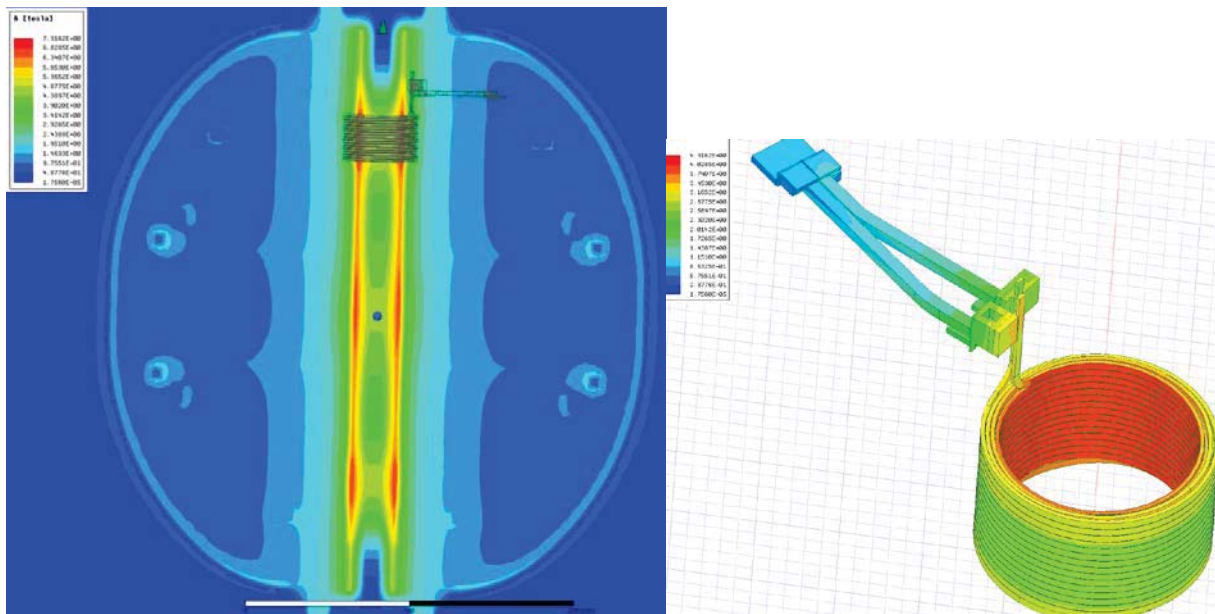


Figure 14 Total Magnetic Fields from EQ #51 on PF1-a upper.

Figures 15-17 present the vertical forces out of all 96 EQ # on the inner PFs – with a comparison of DPSS values. This further validated the PDR results.

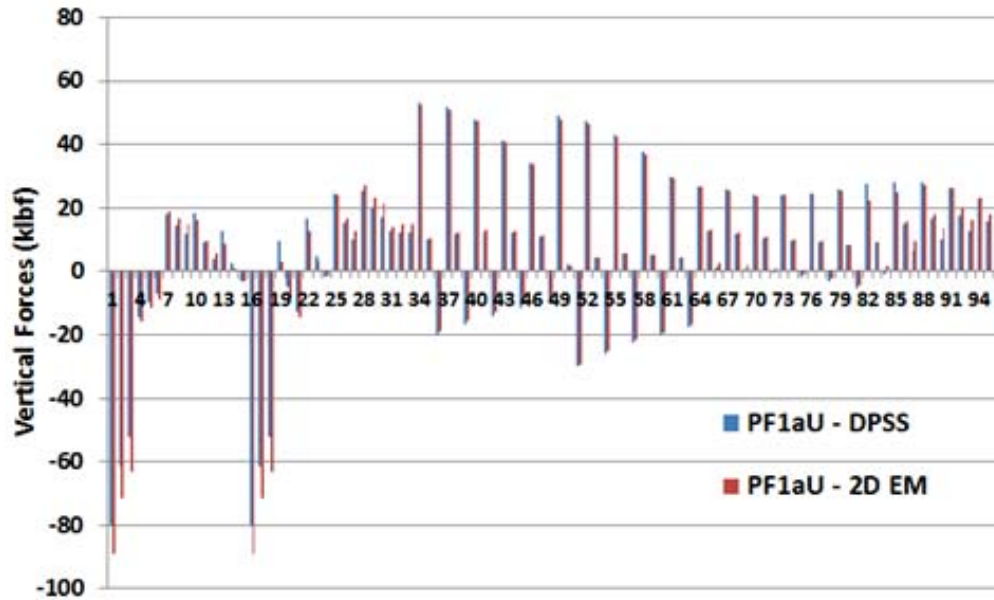


Figure 15 Total Magnetic Fields from EQ #51 on PF1-a upper.

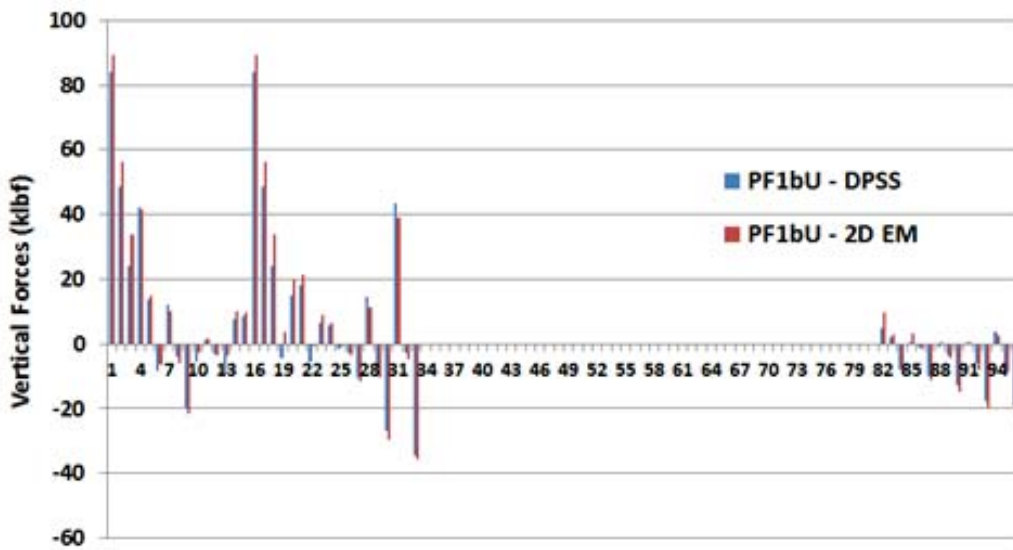


Figure 16 Total Magnetic Fields from EQ #51 on PF1-a upper.

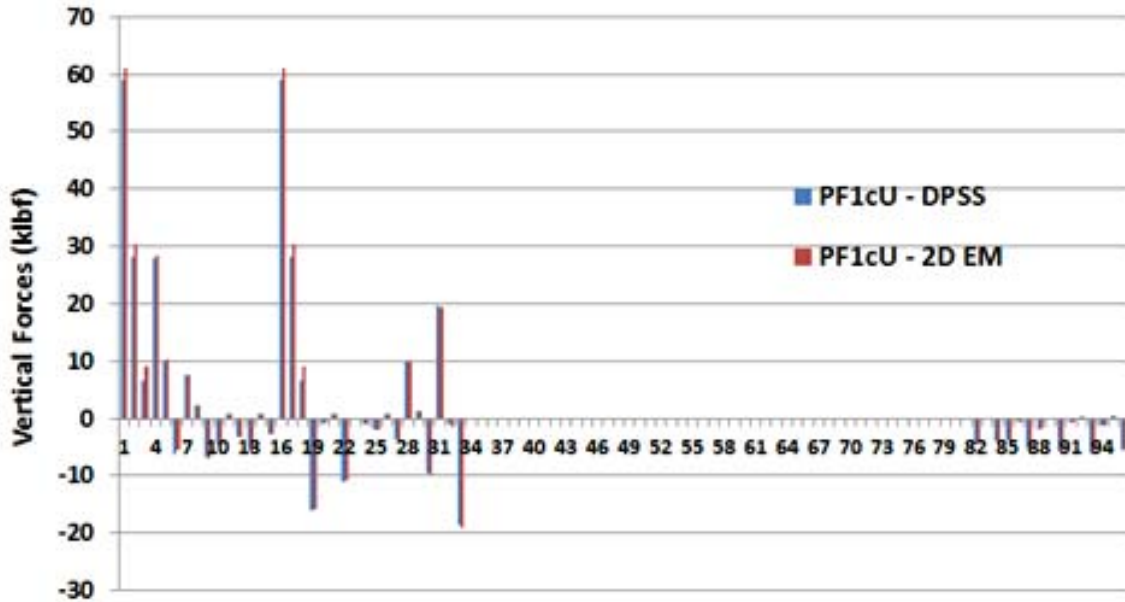


Figure 17 Total Magnetic Fields from EQ #51 on PF1-a upper.

EM Stresses in Conductors when Pulsed

Static structural analysis has been performed based on the resultant Lorentz forces from EM analysis to extract conductor stresses when the coils are pulsed. The typical conductor stresses are shown in Figures 18-19. The results are also summarized in Table 7. The coil design meets the conductor static and fatigue requirements per NSTX-U structural design criteria [4]. The maximum conductor hoop stress is scanned for all 96 EQ scenarios and results are shown in Figure 20 (worst case with 2 MA shaped plasma). The conductor stress meets allowable with less than 42 MPa on the conductor. The resultant EM forces are compared with the Design Point Spreadsheet forces. In general there are only small differences for the large loads that matter. The maximum hoop stress is about 41 MPa which is acceptable. The peak conductor stress (64 MPa) from worst case EQ # and max hoop stress for all 96 EQ scenarios meets the static (93 MPa) and fatigue allowable (125 MPa).

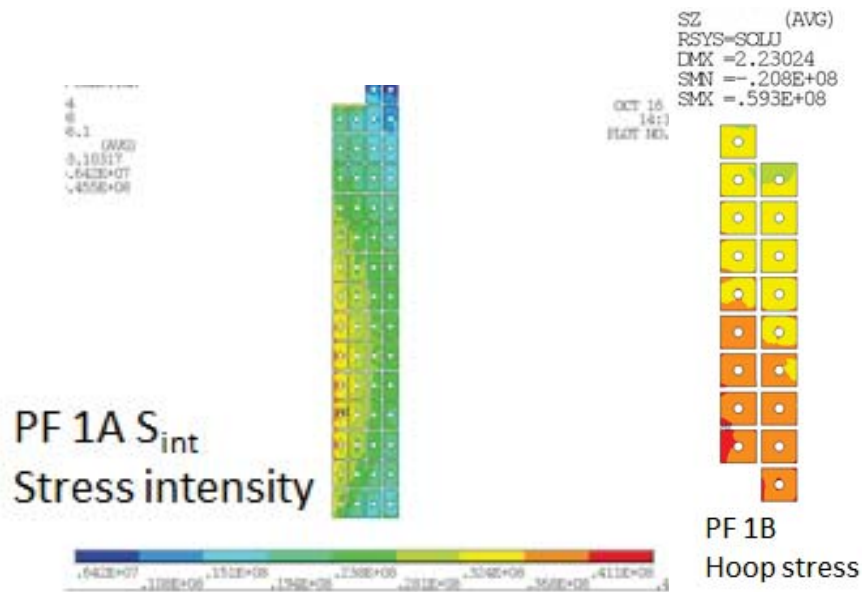


Figure 18 Typical conductor stresses in PF-1a and PF-1b when pulsed

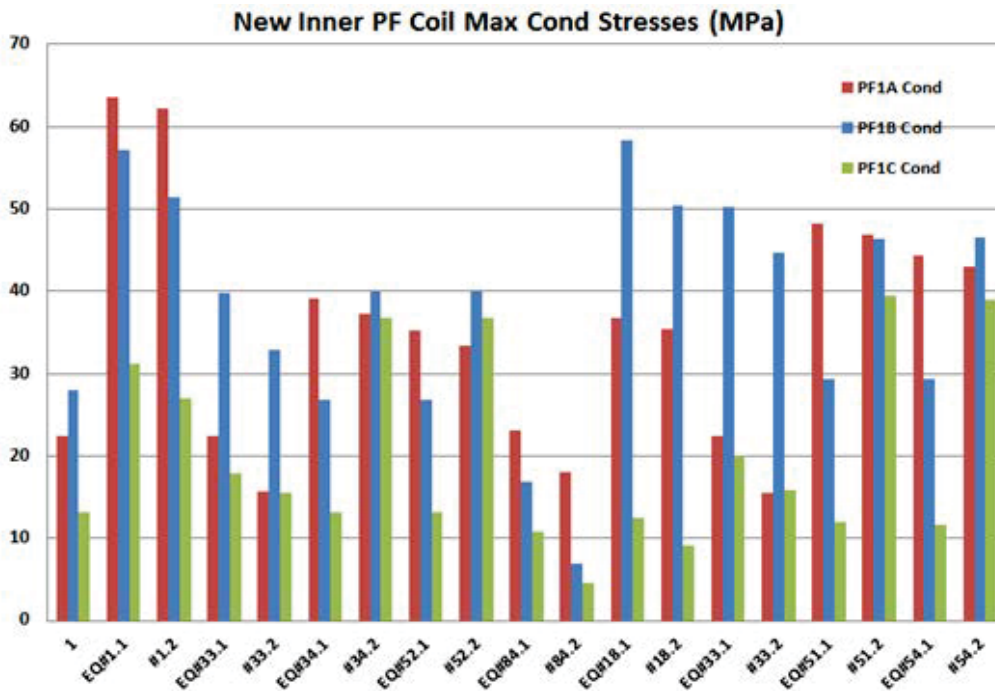


Figure 19 Conductor peak stresses on inner PFs for selected worst case scenarios; 1 – Thermal only (hot at end of pulse, 1.1 – EM load only and 1.2 – EM + Thermal loads

Table 7 – Summary of Conductor EM Stresses

Design Limit (MPa)	PF-1a	Pf-1b	PF-1c
Static	93	64	59
Fatigue	125	64	59

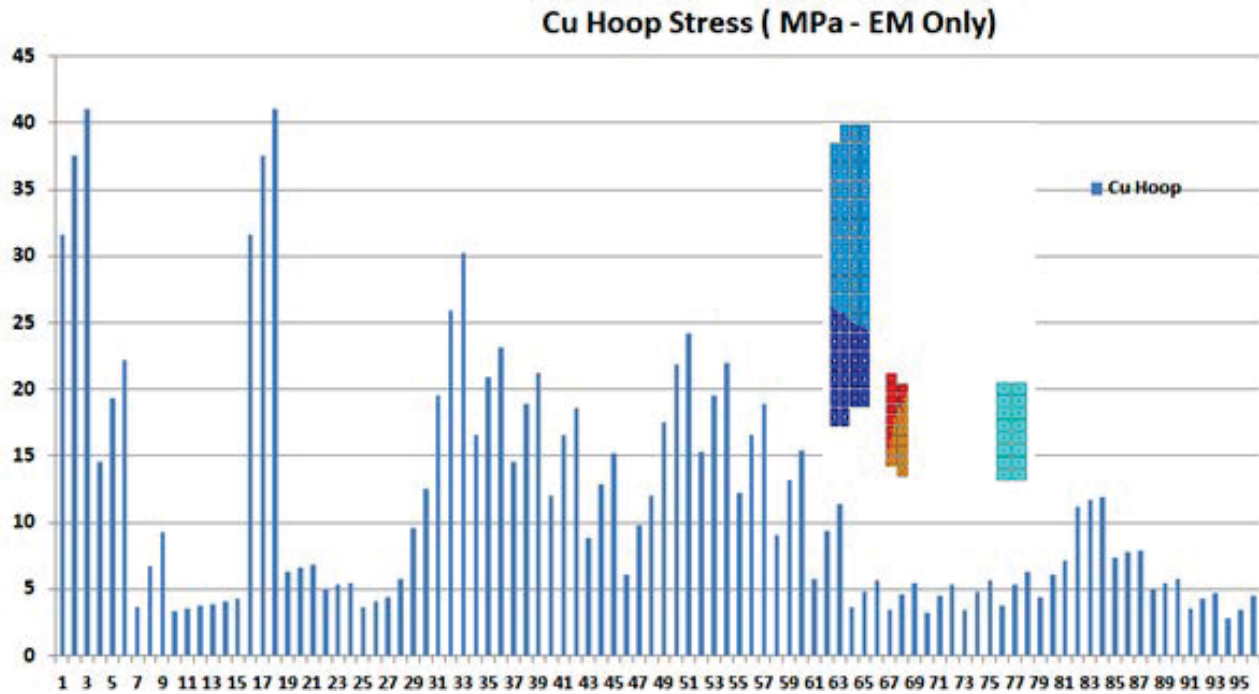


Figure 20 Maximum hoop stresses on inner PF conductors for all 96 EQ scenarios (2 MA shaped plasma)

EM Stress and Strain in Coil Insulations

A critical issue with the coil insulation is the normal tensile strain developed during cool down of the conductors where 10-15 degrees of temperature gradient developed in adjacent turns of conductor in the cooling inlet, the most outer layer of the coil pack. Table 7 presents the summary of insulation EM stress and strain for the inner PFs. The location of the peak stresses in insulation is at the filler blocks. This is not a concern.

Table 8 – Summary of Insulation EM Stress and Strain

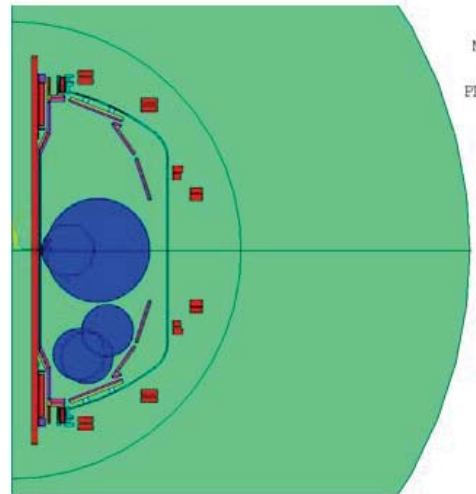
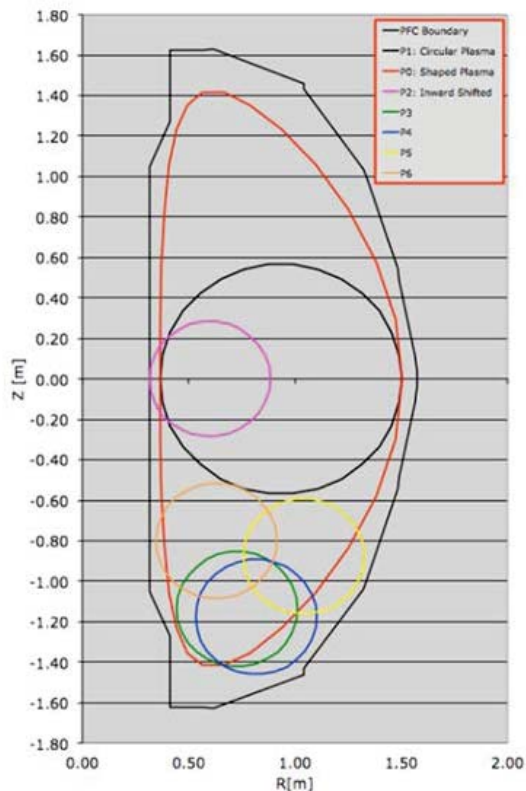
	Design Limit	1A	1B	1C
Compressive stress (MPa)	700	66	65	35
Shear stress (MPa)	14	11	12	9
In-plane strain (%)	+/- 0.5	0.3	0.2	0.05
Tensile strain, normal (%)	0	0	0	0

Disruptions and Post Disruptions – Impact on Inner PFs

Disruptions and post-disruptions are considered as regular events and can happen very frequently according to the Structural Design Criteria, section 2.2.1 [4] and the GRD [1]. Currents in the inner PF coils for the case of post disruptions can be higher than the maximum currents out of the 96 EQ scenarios. This is in fact the case for the PF-1c coils. The estimated over currents for the inner PF-1c is less than 1 kA (<5%) per DPSS [5]. From the stress results on Table 7, there are large margin for the PF-1c coil to cover the <5% over current for the case of post-disruptions (circular or shaped plasma).

As for the PF-1a and PF-1b coils, currents from post-disruptions are less than the maximum currents required from the 96 EQ scenarios. Therefore, no addition analysis is needed.

Normal Loads, Plasma Disruptions

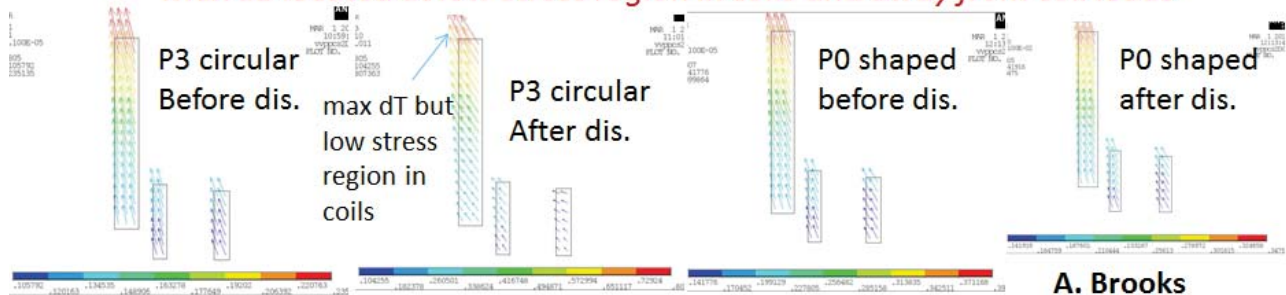


Over Current (kA)	PF-1a	PF-1b	PF-1c	%
Disrupt Circular	-1.9	-0.59	0.2	(-10, 1)
Disrupt Shaped	-0.85	-0.55	0.7	(-4.3, 3.5)

Currents and loads increase only in 1c coils
 Maximum over current is 3.5% for shaped plasma

Normal Loads, Plasma VDEs

- GRD 7 plasma disruption scenarios produce different fields at PF1 coils
 - 6 circular plasmas - 4 VDEs, 1 shifted to CS, 1 mid plane disruption
 - 1 full elongated plasma to disrupt in place
- VV and CS shield PF1 coils from most of disruption effects**
- Field from plasma & eddy current at PF1 mostly affected by VDEs at P3
 - Largest field change (.24 T to .81 T) is from P3 when quenches at PF1*
 - Affect polar region the most on sling structure support*
 - Shaped plasma – insignificant field change (0.4 T to 0.35 T) from P0
 - Max dB located at low stress region in coils and away from coil leads*



The plasma vertical displacement events (VDEs) are defined in the GRD with 7 plasma disruption scenarios producing different fields at the inner PF coil locations. Vacuum vessel and center stack will shield the coils from most of the disruption effects. However, the largest field change may happen from P3 when plasma quenches close to the inner PF coils. This will affect mostly the polar region on the sling structure support (eddy current loading). For the coils, the maximum field change is located near the coil ends (far end of the coil lead region) where stress in the coil winding pack is very low. A factor of safety (stress) more than 3 is expected in this region. Therefore, this VDEs induced field and stress change will not be an issue for the PF1 coils.

Suppress and Bypass Currents and Coil Response

Electrical simulations showed that instantaneous currents during rectifier suppress and bypass may exceed the maximum inner PF coil currents for the 96 EQ scenarios during normal operations. However, the chance of the worst case current transient occurring is low with a probability of less than 0.05% over the lifetime of the machine operations [13]. According to NSTX-U Structural Design Criteria, this is “Unlikely Events” and the design limits can have a multiplier of $k=1.35$ factor. The dynamic amplification factor on

the inner PFs during rectifier suppress and bypass is estimated to be within 1.1-1.2 so the overall stress effects on the inner PFs is within the structural design allowable for the conductors and the coil insulations.

A structural dynamic response calculation also indicated that the Dynamic Load Factor is basically 1.0, which means that we only need to accept the coil current overload as a static load case but can be treated as “Unlikely Events” [14].

Off-Normal, Suppress/Bypass Blip

- **Fault condition triggers coil protection by rectifier suppress & Bypass**
 - Overcurrent on inner PF coils from 2% to 5%
 - Probability of occurrence for 2% over EQ + blip current is 0.05% (*Unlikely*)
 - Probability for 5% over EQ + blip current is 5e-5 (*extremely Unlikely*)
- **Structural Design Criteria K factor**
 - *K = 1.2 for unlikely conditions, K = 1.35 for extremely unlikely conditions*
 - *Evaluation of secondary stress not required*
- **Coil and Bus Structural Dynamic Response to suppress & bypass over-current**
 - Little dynamic amplification from 5% & 0.5% damped cases for coil and bus bars
 - Evaluation of coils can be based on static structural assessment of over currents

	PF-1a		PF-1b		PF-1c	
Current (kA)	20	20	21	21	20	20
Headroom	2% over	5% over	2%	5%	2%	5%
Blip over current	2.84	2.84	3.02	2.98	3.67	3.65
% Blip current	14%	14%	14%	14%	18%	18%

Currents and loads increase less than 20% for unlikely and extremely unlikely events - > ***no impact on coil structural assessment results since 20% and 35% higher allowable***

Conclusion: (*Specify whether or not the purpose of the calculation was accomplished*)

A complete global electromagnetic analysis was performed for the inner PF coils PF-1a, -1b and -1c using 2D axis-symmetric models with winding pack details for the 96 EQ scenarios prescribed in the DPSS [5]. The worst case EQ scenarios for each of the inner PF coils are identified for detailed structural analysis of the winding packs. The maximum local poloidal magnetic fields and the Lorentz forces on inner PFs were extracted for various plasma conditions. The radial and vertical forces are comparable with the DPSS.

The main conclusions include

1. *The conductor static and fatigue stresses meet the NSTX-U structural design limits. The insulation shear and compressive stresses meet the design allowable for all 96 EQ scenarios with additional 10% headroom on the PF coil currents.*
2. *The worst case EQ scenarios in terms of maximum local magnetic fields and stresses in coil winding packs for PF-1a, PF-1b and PF-1c coils are EQ#1 & 51, EQ #33 and EQ #18 respectively.*
3. *Plasma disruptions and post-disruption events, as well as Vertical Displacement Events (VDEs), shall be considered as normal events, only PF-1c coils have 5% overall currents during post-disruptions from the 96 EQ scenarios, which is much lower than the stress margins for the PF-1c coils. The field and stress change due to worst case VDEs will not be an issue for the inner PFs.*

Although the new design with a spiral winding of inner PF solenoids is much better in terms of field symmetry than the previous design with joggles in the winding, the 3D impact of coil spiral winding to net Lorentz forces, error fields, and the magnetic centers is not included in the 2D calculation. A complete 3D analysis using ANSYS MAXWELL has been performed for each of the inner PFs with spiral winding of coils, lead flags and bus bars. The results are reported in the leads and bus bar analysis.